

## PREPARATION AND CHARACTERIZATION OF BISMUTH SULPHIDE NANOCRYSTALLINE THIN FILMS BY CHEMICAL BATH DEPOSITION METHOD IN ACIDIC AQUEOUS MEDIA

A. BEGUM\*, A. HUSSAIN, A. RAHMAN  
*Gauhati University, Guwahati-781014 (India)*

Bismuth sulphide ( $\text{Bi}_2\text{S}_3$ ) nanocrystalline thin films of different molarities (0.2M to 1.0M) were deposited on tinchloride treated glass substrates from an acidic aqueous solution (pH=2.0) of bismuth nitrate and sodium thiosulfate in the presence of ethylenediamine tetraacetic acid (EDTA) at a bath temperature of 333K. The prepared  $\text{Bi}_2\text{S}_3$  thin films were characterized using X-ray diffraction (XRD), X-ray fluorescence (XRF), scanning electron microscopy (SEM), optical absorption spectra and electrical conductivity measurements. The average grain sizes as calculated from Scherrer's formula were found to be within the range 10 nm to 19 nm. With increase in grain size optical band gap energy was found to decrease from 2.57 eV to 2.26 eV. The electrical conductivity measurements of the undoped  $\text{Bi}_2\text{S}_3$  thin films were found to be of the order of  $10^{-6} \Omega^{-1} \text{cm}^{-1}$ .

(Received March 21, 2011, Accepted April 27, 2011)

*Keywords:* Bismuth sulfide, Nanocrystalline, X-ray diffraction, Optical properties, Electrical conductivity

### 1. Introduction

Nanocrystalline semiconductors are of great interest for scientific research due to their important applications in advanced electronic and optoelectronic devices. Bismuth sulfide ( $\text{Bi}_2\text{S}_3$ ) is one of the most attractive semiconducting materials for a wide variety of applications in photovoltaic converters, photodiode arrays, thermoelectric cooling technologies based on the peltier effect [1,2]. The direct band gap value ( $E_g=1.7$  eV) [3] of  $\text{Bi}_2\text{S}_3$  falls in the region of the visible region of energy spectrum and makes it an ideal candidate for solar energy conversion devices.  $\text{Bi}_2\text{S}_3$  is one of the earliest materials known to exhibit photoconducting properties [4]. As compared to methods such as thermal evaporation [5], the hot wall method, hydrothermal synthesis [6], ultrasonic method [7], solvothermal decomposition [8], reactive evaporation [9], spray pyrolysis [10], cathodic and anodic electrodeposition microwave irradiation [11] etc, for the preparation of  $\text{Bi}_2\text{S}_3$  thin films, chemical bath deposition (CBD) method offers the advantages of economy, convenience, large area deposition of thin films at relatively low temperature and pressures [12].

In the present paper, we report the chemical synthesis of nanocrystalline  $\text{Bi}_2\text{S}_3$  thin films using CBD method and characterizations of  $\text{Bi}_2\text{S}_3$  thin films of five different molarities.

---

\*Corresponding author: anayarabegum786@gmail.com

## 2. Experimental

### 2.1 Substrate cleaning and treatment

Glass substrates were cleaned in a mixture of Nitric acid and iso-propyl alcohol. Then they were washed successively with distilled water, iso-propyl alcohol and acetone and dried in an oven at 373K. The cleaned glass substrates were dipped in 0.05 wt% tinchloride for 20 minutes rinsed with distilled water and heated at 473 K in the oven. This treatment of glass substrates is done to initiate heterogeneous nucleation [13] and  $\text{Bi}_2\text{S}_3$  thin film deposition.

### 2.2 $\text{Bi}_2\text{S}_3$ film deposition

For the preparation of  $\text{Bi}_2\text{S}_3$ , bismuth nitrate ( $\text{Bi}(\text{NO}_3)_3$ ) and sodium thiosulfate ( $\text{Na}_2\text{S}_2\text{O}_3$ ) were used as  $\text{Bi}^{3+}$  and  $\text{S}^{2-}$  ions source respectively. Ethylenediamine tetraacetic acid (EDTA) was used as complexing agent for the slow release of  $\text{Bi}^{3+}$  ions in the solution.  $\text{Bi}(\text{NO}_3)_3$  has a strong tendency to hydrolyze, so a 2M solution of nitric acid ( $\text{HNO}_3$ ) was used as its solvent. Using this solvent, 15ml of 0.2M  $\text{Bi}(\text{NO}_3)_3$  solution was prepared and with constant stirring, 12ml of 0.1M of EDTA solution was added to it. To the above mixture 9ml of 0.2M  $\text{Na}_2\text{S}_2\text{O}_3$  solution was added. The pH of this reaction bath was maintained at 2 by slowly adding NaOH solution dropwise. The substrates were vertically immersed in the reaction bath and the temperature of the bath was increased slowly. After attaining 333K, the reaction beaker was kept at room temperature for further deposition. After a deposition period of 12hrs, the substrates were taken out, rinsed in distilled water and dried. Five different molarities of  $\text{Bi}(\text{NO}_3)_3$  (0.2M, 0.4M, 0.6M, 0.8M and 1.0M) were used to deposit  $\text{Bi}_2\text{S}_3$  thin films.

### 2.3 Characterization of $\text{Bi}_2\text{S}_3$ thin films

The thickness of the  $\text{Bi}_2\text{S}_3$  thin films was measured by multiple beam interferometer technique. To study the crystallographic properties of the prepared  $\text{Bi}_2\text{S}_3$  films, X-ray diffraction analysis was carried out using X-ray diffractometer (PW 1830) at room temperature. Surface morphological studies of chemically deposited  $\text{Bi}_2\text{S}_3$  thin films were done using Scanning Electron Microscope (JEOL JSM 6360). X-ray fluorescence study (XRFS) was done using AXIOS Spectrometer (DY 840) for elemental analysis of the as-prepared films and optical absorption studies were carried out using a UV-visible spectrophotometer (VARIAN CARY 300 scan) in the wavelength range 360 nm-900 nm.

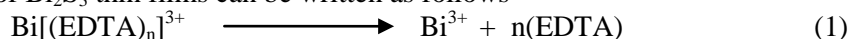
The electrical conductivity measurements of the films were done using two coplaner Aluminium (Al) electrodes separated by a small gap. These were vacuum evaporated at the two ends of the rectangular  $\text{Bi}_2\text{S}_3$  strip. The evaporation of electrodes was performed at a reduced pressure of  $10^{-5}$  Torr in a vacuum evaporation unit (VICO-12). The conductivity of  $\text{Bi}_2\text{S}_3$  was determined by measuring the resistance of the samples using an electrometer (Keithley 6514) in the temperature range 298K to 383K and the same temperature was varied using a temperature controller. Temperature of the samples was measured by means of a thermocouple.

## 3. Results and discussion

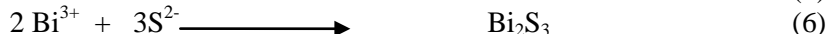
### 3.1 Film growth

The deposition process of  $\text{Bi}_2\text{S}_3$  is based on the slow release of  $\text{Bi}^{3+}$  and  $\text{S}^{2-}$  ions in the solution which then condenses ion by ion basis on the substrates. Deposition of  $\text{Bi}_2\text{S}_3$  thin films occurs when the ionic product of  $\text{Bi}^{3+}$  and  $\text{S}^{2-}$  ions exceeds the solubility product of  $\text{Bi}_2\text{S}_3$ . The concentration of  $\text{Bi}^{3+}$  and  $\text{S}^{2-}$  ions in the solution controls the rate of  $\text{Bi}_2\text{S}_3$  formation. The rate of

$\text{Bi}^{3+}$  ions is controlled by EDTA, which forms a complex  $\text{Bi}[(\text{EDTA})_n]^{3+}$  with  $\text{Bi}^{3+}$  [14]. The reaction for the formation of  $\text{Bi}_2\text{S}_3$  thin films can be written as follows



In acidic medium dissociation of  $\text{S}_2\text{O}_3^{2-}$  takes place as,



### 3.2 XRD study

X-ray diffractograms of the  $\text{Bi}_2\text{S}_3$  thin films of 0.2M and 1.0M are shown in Fig. 1. The broad hump in the XRD pattern is due to amorphous glass substrates [14]. Calculation of interplanar distance ( $d_{\text{hkl}}$ ) values by considering the peak count and background count indicated presence of various planes of  $\text{Bi}_2\text{S}_3$  which showed good matching with the JCPDS card 17-320. The prominent peaks with the corresponding planes are shown in the figures. The peak at  $2\theta$  value of  $21^\circ$  in case of 1.0M  $\text{Bi}_2\text{S}_3$  film may correspond to some intermediate compound formed during the reaction. The average crystallite size  $D$ , was calculated using Scherrer's formula [15],

$$D = \frac{k\lambda}{\beta \cos \theta} \quad (7)$$

where  $k$  is a constant taken to be 0.94,  $\lambda$  the wavelength of the of X-ray used ( $\lambda=1.5406\text{\AA}$ ) and  $\beta$  the full width at half maximum intensity of the peak and  $\theta$  is the Bragg's angle. The average grain size of  $\text{Bi}_2\text{S}_3$  thin films of different molarities are given in table1. The average grain size is found to increase from 10 nm to 19 nm as the molarities was increased from 0.2M to 1.0M.

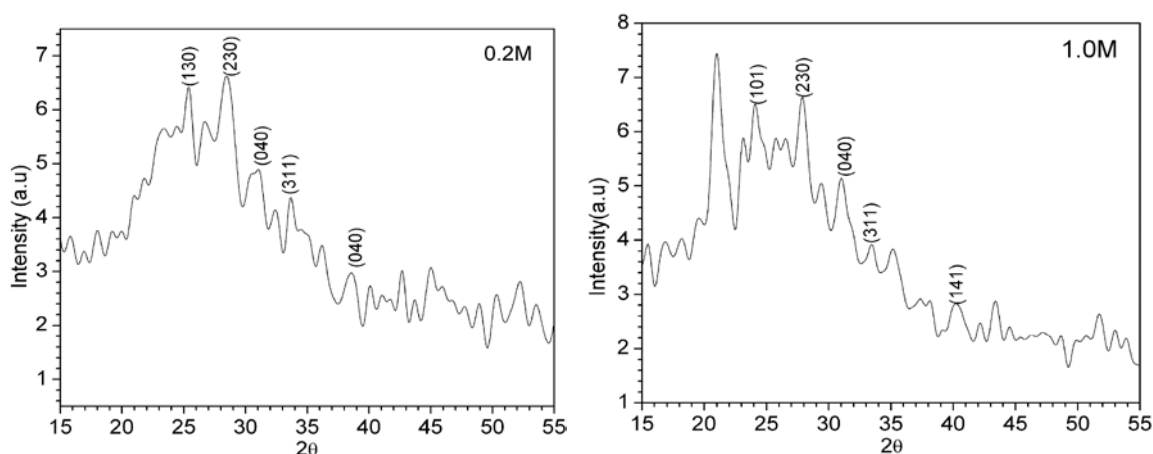


Fig. 1. X-ray diffraction patterns of 0.2M and 1.0M  $\text{Bi}_2\text{S}_3$  thin films .

### 3.3 Scanning electron microscope analysis

Fig.2. shows SEM micrograph of  $\text{Bi}_2\text{S}_3$  thin film of 1M which was used for the study of surface morphology. The films were found uniform and continuous and without any visible pores or cracks.

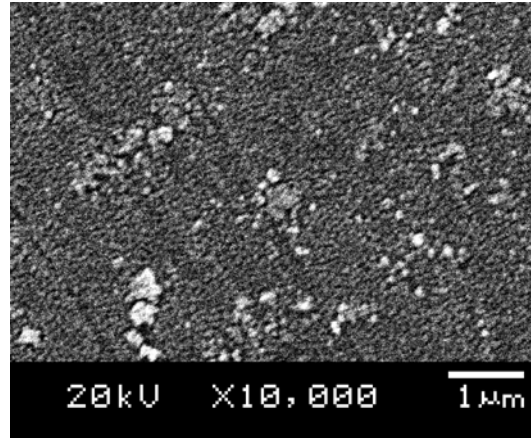


Fig. 2. SEM image of 1.0M  $\text{Bi}_2\text{S}_3$  thin film.

### 3.4 X-ray Fluorescence (XRF) studies

Fig.3. shows the XRF spectra of  $\text{Bi}_2\text{S}_3$  thin films of 0.2M. The spectrum exhibits the prominent peaks of BiMB, BiMA1 and S KA lines showing the presence of Bi and S in the prepared film. The spectrum shows a peak of ClKA which may be due to probable impurities present in the glass substrates.

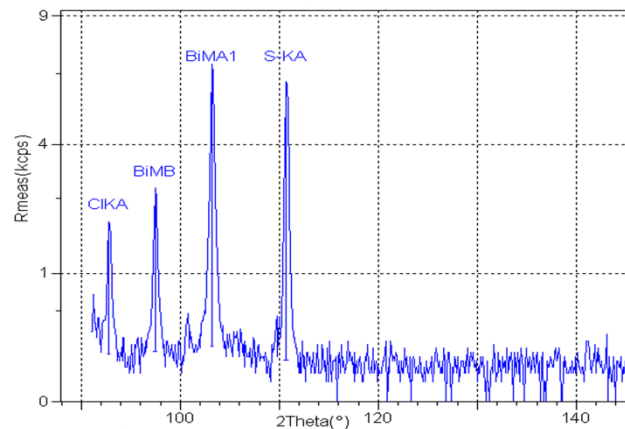


Fig. 3. XRF spectra of 0.2M  $\text{Bi}_2\text{S}_3$  thin film

### 4. Optical Absorption studies

The optical absorption spectra of  $\text{Bi}_2\text{S}_3$  thin films of five different molarities are shown in Fig.4. The optical absorption edge showed a red shift with increase in molarities. The relationship between the absorption coefficient  $\alpha$  and the incident photon energy can be written as [16, 17]

$$\alpha = \frac{a(h\nu - E_g)^n}{h\nu} \quad (8)$$

Where “a” is a constant,  $E_g$  is the band gap, n is a constant equal to  $\frac{1}{2}$  for direct bad gap semiconductor and 2 for indirect bad gap semiconductor. The value of  $\alpha$  is obtained from the relation [18]

$$\alpha = 2.303 \frac{A}{t} \quad (9)$$

where ‘A’ is the absorbance and ‘t’ is the thickness of the film.

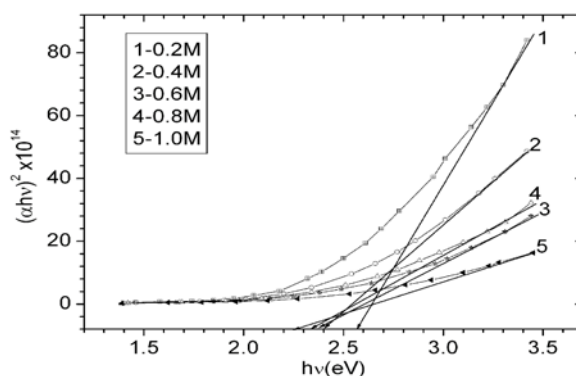


Fig. 4. UV-Absorption spectra of  $\text{Bi}_2\text{S}_3$  thin films.

The variation of  $(\alpha hv)^2$  versus  $(hv)$  plot (Fig.5.) for the prepared  $\text{Bi}_2\text{S}_3$  thin films is linear at the absorption edge which confirms that  $\text{Bi}_2\text{S}_3$  is a direct band gap semiconductor. The band gap energies were obtained from extrapolating the straight portion of the  $(\alpha hv)^2$  versus  $(hv)$  plot on the  $(hv)$  axis at

$$(\alpha hv)^{1/n} = 0 \quad [19] \quad (10)$$

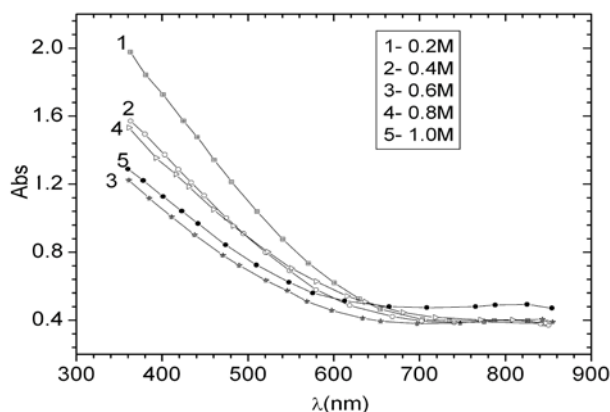


Fig. 5.  $(\alpha hv)^2$  vs  $(hv)$  plots of  $\text{Bi}_2\text{S}_3$  thin films.

It was found that the band gap changed from 2.56 to 2.27eV as molarities varied from 0.2M to 1.0M. As the molarities were increased, the grain size of  $\text{Bi}_2\text{S}_3$  thin films was increased resulting in decrease in band gap. This is due to the quantum size effect observed in nanocrystalline thin films of semiconductors. Similar ‘blue/red shift’ in band gap energy values with thickness and grain size have been reported earlier for chemically prepared  $\text{Bi}_2\text{S}_3$  thin films [14, 20].

## 5. Electrical conductivity

The variation of  $\log \sigma$  vs  $1/T$  of  $\text{Bi}_2\text{S}_3$  thin films measured in the 298K-383K temperature range is shown in Fig.6. All the samples show two regions in the curve. As the temperature is increased, the conductivity is observed to remain constant initially and after attaining about 313K, it increases continuously. We have found average activation energy about 0.6 eV. There was no activation at low temperature till 313K, above which, electrons were available from the level at 0.6 eV and increase in conductivity was observed.

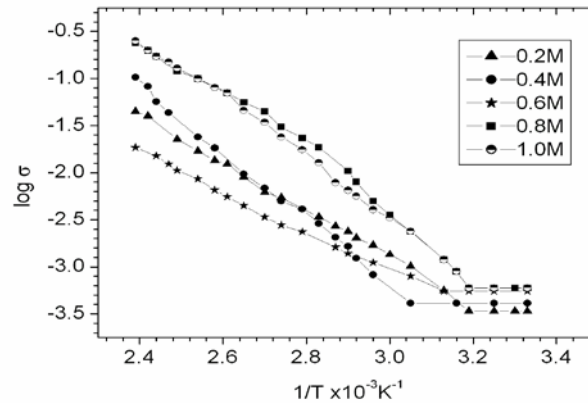


Fig. 6. Variation of  $\log(\sigma)$  vs  $1/T$  for  $\text{Bi}_2\text{S}_3$  thin films.

The room temperature conductivity of the  $\text{Bi}_2\text{S}_3$  thin films is of the order of  $10^{-6} \Omega^{-1}\text{cm}^{-1}$ . Grain boundary discontinuity and thickness of the films may be responsible for the high resistance of the  $\text{Bi}_2\text{S}_3$  films. It was found that with increase in molarities, hence grain size; there was increase in the room temperature conductivity of the samples. The activation energy was estimated using the relation,

$$\sigma = \sigma_0 \exp \frac{E_a}{2kT}$$

(11)

where  $E_a$  is activation energy,  $\sigma_0$  is a constant,  $k$  is Boltzmann's constant and  $T$  is absolute temperature. The values of room temperature conductivity and activation energy are tabulated in table 1. Increase in conductivity and decrease in activation energies for  $\text{Bi}_2\text{S}_3$  films on increasing the molarities is due to increase in grain size of  $\text{Bi}_2\text{S}_3$  films.

Table1. Electrical conductivity and activation energy values of  $\text{Bi}_2\text{S}_3$  thin films of different molarities.

Molarity	Grain size (nm)	Band gap energy (eV)	Room temperature conductivity $10^{-6} \times (\Omega^{-1}\text{cm}^{-1})$	Activation Energy (eV)
0.2	10	2.57	3.39	0.68
0.4	13	2.40	4.11	0.67
0.6	15	2.38	5.52	0.64
0.8	17	2.34	5.97	0.60
1.0	19	2.26	6.34	0.54

## 6. Conclusion

From the present studies, it is concluded that  $\text{Bi}_2\text{S}_3$  thin films of five different molarities prepared by CBD are found to be nanocrystalline with grain size within the range 10 nm to 19 nm. The grain size of  $\text{Bi}_2\text{S}_3$  thin films are found to increase with increase in molarity. Consequently, optical band gap energy was decreased and electrical conductivity was increased with increase in molarities.

## Acknowledgement

We express our gratefulness to the Department of USIC, Gauhati University, Guwahati and SAIF, NEHU for providing us the XRD, XRF and SEM facilities respectively.

## References

- [1] B. Miller, A.Heller, Nature **262**, 680 (1976).
- [2] O.Robin, J.M.Grimm, G.Wojtkiewicz, R. Weissleder, Nat. Mater. **5**, 118 (2006).
- [3] R.S.Mane, B.R. Sankapal, Thin Solid Films **359**, 136 (2000).
- [4] R.H. Bube, Photoconductivity of Solids, Krieger Publ. Co., New York, 1978.
- [5] M.E. Rincon, M. Sanchez, P.J. George, A. Sanchez, P.K. Nair, J. Solid State Chem. **136**, 167 (1998).
- [6] M.W. Shao, M.S. Mo, Y. Cui, G. Chen, Y.T. Qian, J.Crystal Growth **233**, 799 (2001).
- [7] S.Y. Wang, Y.W. Du. J.Crystal Growth **236**, 627 (2002).
- [8] S.H. Yu, L. Shu, J.A. Yang, Z.H. Han, Y.T. Qian, Y.H. Zhang, J. Mater Res. **14**, 4157 (1999)
- [9] J. Lukose, d B. Pradeep, Solid State Commun. **78**, 535 (1991).
- [10] V.V.Killedar, C.D.Lokhande, C.H.Bhosale, Thin Solid Films **289**, 14(1996).
- [11] X.H. Liao, J.J. Zhu, H.Y. Chen, Mater Sci. Eng. B **85**, 85 (2001).
- [12] R.S.Mane, C.D.Lokhande, Mater. Chem. Phys. **65**, 1 (2000).
- [13] B.Pejova, I.Grozdanov, Mater. Chem. Phys. **99**, 39 (2006).
- [14] R.S.Mane, B.R.Sankapal, C.D.Lokhande, Mater. Res. Bull. **35**, 587 (2000).
- [15] B.D.Cullity, Elements of X-ray diffraction, 2<sup>nd</sup> edition, Addison-Wisley Publishing Company, Inc. USA (1978).
- [16] P.K.Ghosh, S.Jana, U.N.Maity, K.K.Chattopadhyay, Physica E. **35**, 178 (2006).
- [17] F.I.Ezema, A.B.C.Ekwealor, R.U.Osigi, Turk. Journ.Phys. **30**, 157 (2006).
- [18] J.Barman, K.C.Sarma, M.Sarma, K.Sarma, Indian J. Pure Appl. Phys. **46**, 333 (2008).
- [19] D.O.Eya, Pacific Journal of Science and Technology **7**, 2 (2006).
- [20] C.D.Lokhande, A.U.Ubale, P.S.Patil, Thin Solid Films **302**, 1 (1997).